

Structural Defects within the Carbamate Tunnel of Carbamoyl Phosphate Synthetase[†]

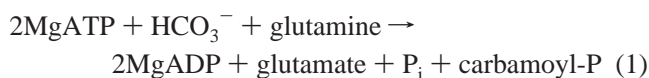
Jungwook Kim, Stanley Howell, Xinyi Huang, and Frank M. Raushel*

Department of Chemistry, Texas A&M University, P.O. Box 30012, College Station, Texas 77843-3012

Received June 18, 2002; Revised Manuscript Received August 16, 2002

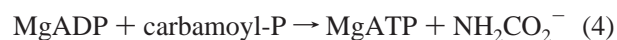
ABSTRACT: The X-ray crystal structure of carbamoyl phosphate synthetase (CPS) from *Escherichia coli* has unveiled the existence of two molecular tunnels within the heterodimeric enzyme. These two interdomain tunnels connect the three distinct active sites within this remarkably complex protein and apparently function as conduits for the transport of unstable reaction intermediates between successive active sites. The operational significance of the *ammonia tunnel* for the migration of NH₃ is supported experimentally by isotope competition and protein modification. The passage of carbamate through the *carbamate tunnel* has now been assessed by the insertion of site-directed structural blockages within this tunnel. Gln-22, Ala-23, and Gly-575 from the large subunit of CPS were substituted by mutagenesis with bulkier amino acids in an attempt to obstruct and/or hinder the passage of the unstable intermediate through the carbamate tunnel. The structurally modified proteins G575L, A23L/G575S, and A23L/G575L exhibited a substantially reduced rate of carbamoyl phosphate synthesis, but the rate of ATP turnover and glutamine hydrolysis was not significantly altered. These data are consistent with a model for the catalytic mechanism of CPS that requires the diffusion of carbamate through the interior of the enzyme from the site of synthesis within the N-terminal domain of the large subunit to the site of phosphorylation within the C-terminal domain. The partial reactions of CPS have not been significantly impaired by these mutations, and thus, the catalytic machinery at the individual active sites has not been functionally perturbed.

Carbamoyl phosphate synthetase (CPS)¹ is a heterodimeric enzyme ($\alpha\beta$), composed of unequal sized subunits with molecular weights of 42 000 and 118 000 (Figure 1). CPS catalyzes the synthesis of carbamoyl phosphate from bicarbonate, ATP, and glutamine/ammonia as summarized in eq 1, and the individual chemical events are depicted in Scheme 1 (1).



The small subunit contains the binding site for glutamine, where it is hydrolyzed to glutamate and ammonia. The larger subunit harbors two ATP binding sites within two homologous domains. The *carboxy phosphate domain* within the N-terminal half of the protein (residues 1–400) is responsible for the phosphorylation of bicarbonate, whereas the *carbamoyl phosphate domain* within the C-terminal half of the

large subunit (residues 553–933) is utilized for the phosphorylation of the carbamate intermediate. In addition to the overall reaction, CPS also catalyzes three partial reactions as shown in eqs 2–4 (2).



The X-ray crystal structure of CPS from *Escherichia coli* unveiled the existence of a molecular tunnel that is ~ 100 Å in length that connects three distinct active sites within the protein (3). This remarkable structural feature has been proposed to be a molecular conduit for the transport of reactive intermediates between successive active sites. The ammonia that is produced at the active site of the small subunit migrates through the *ammonia tunnel* to the large subunit where it reacts with the carboxy phosphate intermediate to form carbamate. The carbamate intermediate then traverses through the *carbamate tunnel* where it is subsequently phosphorylated by the second ATP to form carbamoyl phosphate. The direct diffusion of ammonia from the small subunit to the large subunit has been supported by the dominant incorporation of *internal* ammonia (derived from the hydrolysis of [¹⁴N]glutamine) relative to *external* am-

[†] This work was supported in part by the National Institutes of Health (Grant DK 30343) and the Robert A. Welch Foundation (Grant A-840). S.H. was supported by the NSF-REU program (CHE-0071889).

* To whom correspondence should be addressed. Fax: (979) 845-9452. E-mail: raushel@tamu.edu.

¹ Abbreviations: CPS, carbamoyl phosphate synthetase; GPATase, glutamine phosphoribosylpyrophosphate amidotransferase; PRPP, phosphoribosylpyrophosphate; G3P, glyceraldehyde 3-phosphate; IGP, indole 3-glycerol phosphate; PRA, phosphoribosylamine.

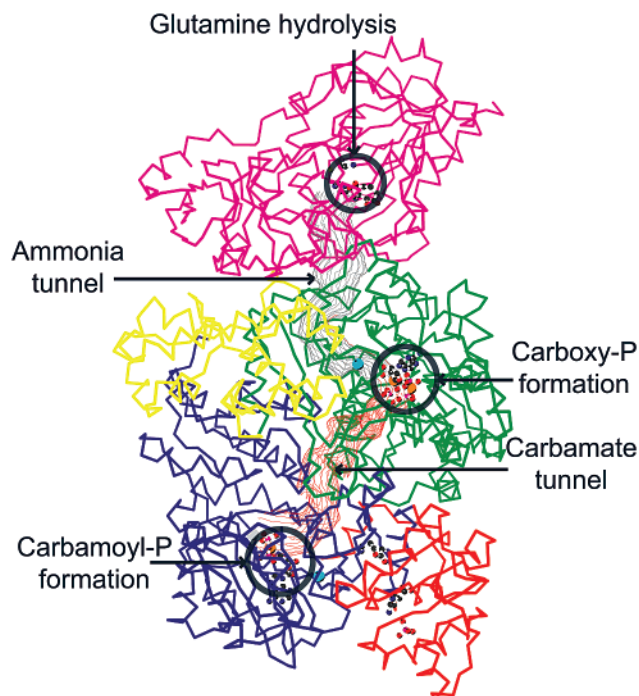
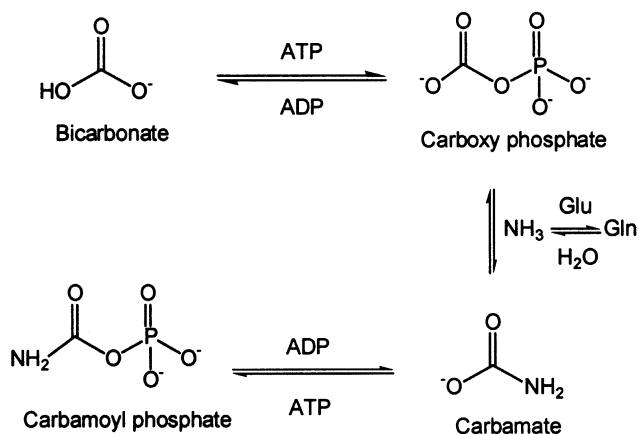


FIGURE 1: α -Carbon trace of the three-dimensional structure of CPS from *E. coli*. Active sites are highlighted as circles. The ammonia tunnel is displayed in gray, and the carbamate tunnel is in bright red. The small subunit is represented in magenta, and the four major domains of the large subunit are displayed according to the following color scheme; the carboxy phosphate domain in green, the carbamoyl phosphate domain in blue, the oligomerization domain in yellow, and the allosteric domain in red. The structure was obtained from Thoden et al. (3).

Scheme 1



monia (from $^{15}\text{NH}_4^+$) into the final product, carbamoyl phosphate (4). More direct evidence for the channeling of ammonia has been provided by the construction of mutants designed to block the tunnel. Specific residues within the interior wall of the molecular tunnel for ammonia were sequentially mutated to bulkier amino acids in an attempt to hinder and retard the passage of ammonia from the site of production to the site of utilization (5, 6). The catalytic properties of two mutant enzymes, G359Y and G359F, were consistent with the restricted transport or leakage of ammonia through the tunnel.

Channeling of the carbamate intermediate between the two phosphorylation domains has been experimentally supported by the absence of isotope incorporation from solvent into

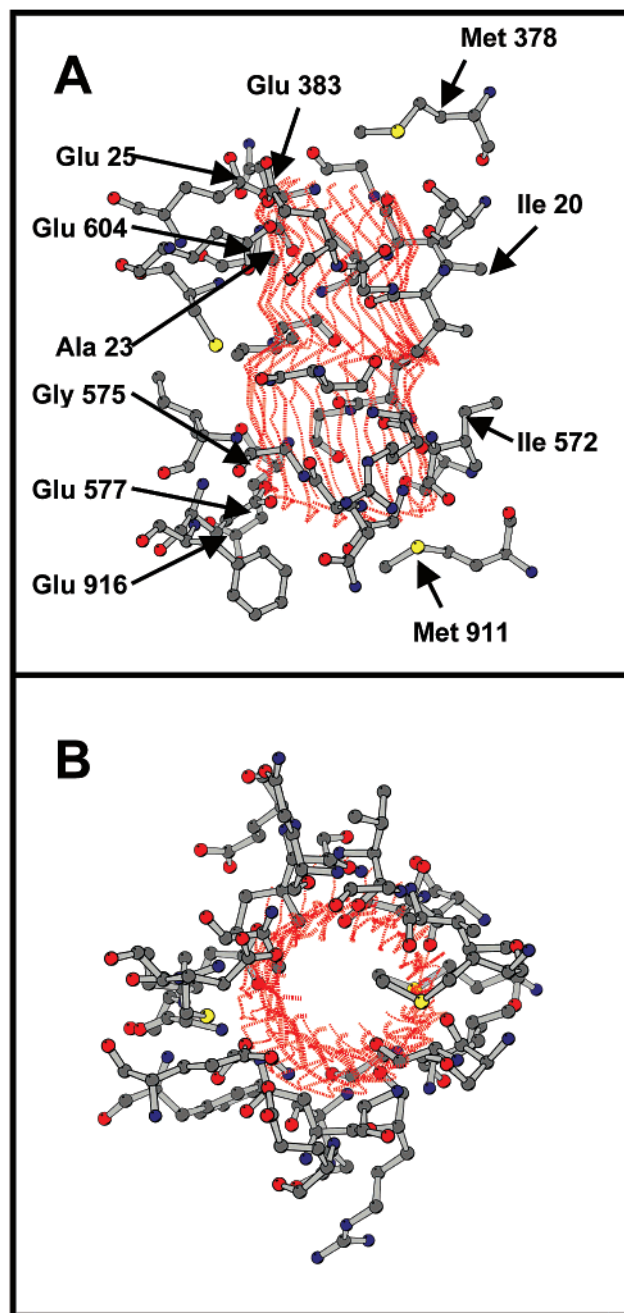


FIGURE 2: Central core of the carbamate tunnel. The trace of the molecular tunnel is highlighted in bright red. (A) Side view of the carbamate tunnel where the top is near the active site within the carboxy phosphate domain and the bottom is adjacent to the active site within the carbamoyl phosphate domain. (B) View through the carbamate tunnel from the carboxy phosphate domain toward the carbamoyl phosphate domain. Coordinates were obtained from Thoden et al. (3).

bicarbonate during the synthesis of carbamoyl phosphate (7). The reported half-life of carbamate at neutral pH is ~ 70 ms (8). Therefore, the protection of this labile intermediate from solvent decomposition is critical for the efficient synthesis of carbamoyl phosphate. However, the functional significance of the carbamate tunnel for the stabilization and transport of carbamate has not been demonstrated experimentally. The overall shape of the carbamate tunnel, which is located directly between the two homologous active sites within the large subunit, is illustrated in Figure 2. Half of the 30 residues that come together to form the core of the carbamate tunnel

originate from the carboxy phosphate domain. The remaining 15 amino acids are from the carbamoyl phosphate domain. The average diameter of the tunnel is ~ 4 Å, and the distance between the two active sites is ~ 31 Å. In this paper, we have probed the direct transport of carbamate through the molecular tunnel that connects the two active sites within the large subunit by the construction and characterization of site-directed mutants. These alterations to the protein structure were intended to obstruct the carbamate tunnel and impede the delivery of carbamate from the carboxy phosphate domain to the carbamoyl phosphate domain within the large subunit of CPS.

MATERIALS AND METHODS

Materials. All chemicals and coupling enzymes were purchased from either Sigma or Aldrich, unless otherwise stated. Restriction enzymes were purchased from New England Biolabs, and *pfu* DNA polymerase was acquired from Promega. The clone for ornithine transcarbamoylase was a generous gift from the laboratory of N. Allewell.

Mutagenesis and Protein Purification. Site-directed mutagenesis of CPS was performed as described previously (9). Oligonucleotide synthesis and DNA sequencing reactions were performed by the Gene Technology Laboratory, Texas A&M University. The plasmids containing the *carAB* genes were transformed in the RC50 cell line of *E. coli* for expression of the wild-type and mutant forms of CPS. The wild type and mutant variants of CPS were purified as previously described (10).

Kinetic Measurements and Analysis. The rate of ADP formation was measured using a pyruvate kinase/lactate dehydrogenase coupling system in the presence of the allosteric activator ornithine (10). The rate of ATP synthesis was measured with a hexokinase/glucose-6-phosphate dehydrogenase coupling system in the presence of ornithine (9). The synthesis of carbamoyl phosphate was assessed by measuring the rate of citrulline formation in a coupled assay containing ornithine transcarbamoylase and ornithine (11). The kinetic parameters were determined by fitting the experimental data to eq 5, where k_{cat} is the turnover number, K_m is the Michaelis constant, and A is the substrate concentration. The data for the enhancement of ATP hydrolysis in the presence of a nitrogen source were fitted to eq 6 (12). In this equation, V_o is the turnover number in the absence of a nitrogen source I (ammonia or glutamine), K_a is the apparent activation constant, and α is the ratio of the velocities in the presence and absence of a nitrogen source. In this case, k_{cat} is expressed as αV_o .

$$v/E_t = (k_{\text{cat}}A)/(K_m + A) \quad (5)$$

$$v/E_t = V_o(K_a + \alpha I)/(K_a + [I]) \quad (6)$$

RESULTS AND DISCUSSION

Carbamate Tunnel. A molecular tunnel connects the two active sites contained within the carboxy phosphate and carbamoyl phosphate domains of the large subunit of CPS. The length of the tunnel, as measured by the distance between the γ -phosphoryl groups of the bound substrate analogue, AMP-PNP, within each of these domains, is ~ 31

Table 1: Sequence Alignment of Homologous Residues that Compose the Carbamate Tunnel in *E. coli*^a

N-terminal domain	C-terminal domain
Ile-18	Asn-570
Val-19	Arg-571
Ile-20	Ile-572
Gly-21	Gly-573
Gln-22	Gln-574
Ala-23	Gly-575
Cys-24	Ile-576
Glu-25	Glu-577
Phe-26	Phe-578
Ala-52	Glu-604
Met-378	Met-911
Ser-380	Ser-913
Val-381	Thr-914
Gly-382	Gly-915
Glu-383	Glu-916

^a Residues in bold are >96% conserved among 61 prokaryotic organisms.

Å (13). The interconnecting tunnel is approximately linear in shape and is capped at each end by Arg-306 and Arg-848. The side chains of these two residues interact with the substrate through ion pair formation with the γ -phosphoryl group of the bound nucleotides. The central core of the carbamate tunnel is composed of 30 residues, where one-half of the amino acids originate from the carboxy phosphate domain and the remaining residues are from the carbamoyl phosphate domain. The identity of the residues that come together from each domain to form the carbamate tunnel is presented in Table 1. The tunnel is reasonably symmetrical in both amino acid composition and geometrical shape from end to end (Figure 2). The diameter of the tunnel entrance near the carboxy phosphate domain is ~ 4.0 Å and then narrows at a point near the intersection of Ala-23 and Val-381 where the diameter is ~ 3.3 Å. The exit at the C-terminal end of the carbamate tunnel has a diameter of ~ 4.5 Å.

The residues that line the interior of the central core of the carbamate tunnel are predominantly nonionic amino acids, except for five glutamates and a lone arginine. However, the guanidinium group of Arg-571 is located outside of the carbamate tunnel. In contrast, the side chain carboxylate groups of the five glutamic acid residues form part of the interior wall of the carbamate tunnel (Figures 3 and 4). Glu-25, Glu-383, and Glu-604 are situated inside the carbamate tunnel entrance near the active site within the carboxy phosphate domain, whereas Glu-577 and Glu-916 are located at the opposite end of the tunnel. Moreover, all of these glutamate residues are found on one side of the interior wall of the carbamate tunnel, rather than randomly dispersed (Figure 4). The opposite wall of the interior tunnel space bears no significant charge, as expected from the nonpolar amino acid composition. It is unclear how the unusual charge distribution within the tunnel interior facilitates the stabilization of the carbamate intermediate as it passes from one end of the tunnel to the other. Carbamate is very unstable at low pH, and thus, protonation of the intermediate must be avoided to prevent an uncoupling of the individual reaction sites from one another (14). Two arginine residues, Arg-306 and Arg-848, are found at the extreme ends of the carbamate tunnel. The side chains of these two residues may act as gatekeepers that regulate the entry and exit of carbamate through the molecular pas-

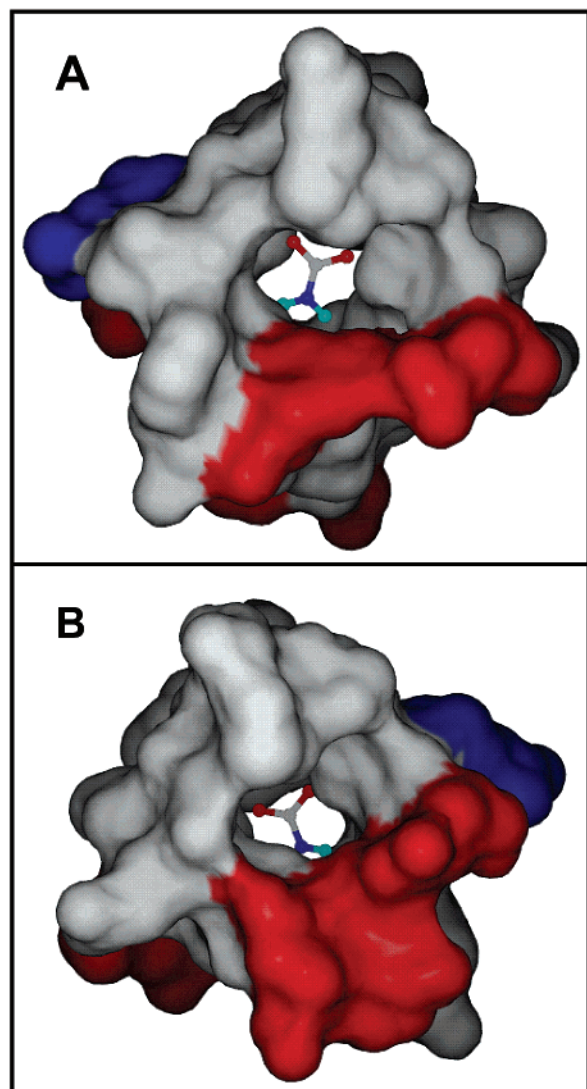


FIGURE 3: Surface representation of the carbamate tunnel with the superposition of carbamate. The surface is colored according to the underlying atoms: red for oxygen and blue for nitrogen. The same color scheme is used for carbamate, but the hydrogens are depicted in light blue. Superposition of carbamate within the tunnel has been modeled using Insight II, and the surface rendering has been achieved using the computer program SPOCK. (A) View from the carbamoyl phosphate domain looking toward the carboxy phosphate domain. (B) View from the carboxy phosphate domain looking toward the carbamoyl phosphate domain.

sageway prior to the formation of the ultimate product, carbamoyl phosphate.

Conservation of Interior Tunnel Residues. The amino acids that constitute the interior walls of the carbamate tunnel are highly conserved among bacteria, plants, and animals (Tables 1 and 3). The five glutamate residues are fully conserved in *E. coli*, human, fruit fly, yeast, and *Arabidopsis*. In addition to the five highly conserved glutamates, the amino acids whose side chains point toward the tunnel interior also appear to be highly conserved (Ala-23, Met-378, and Met-911). There are also five glycine residues that constitute part of the carbamate tunnel, all of which are highly conserved among prokaryotes.

Structural Blockages within the Carbamate Tunnel. The channeling of the carbamate intermediate through the interior

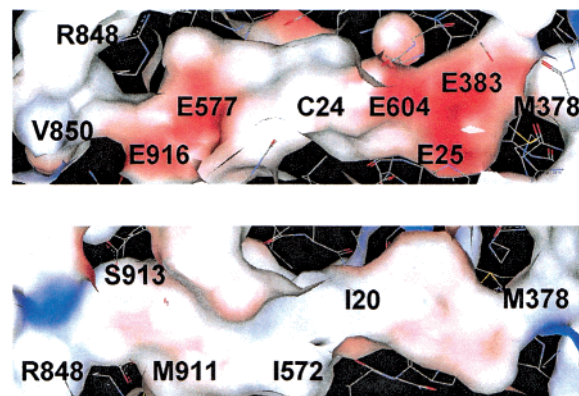


FIGURE 4: Surface representation of the inner wall of the carbamate tunnel. The surface is colored according to the electrostatic charges where red represents negative charge and blue positive charge. This figure was generated using the program Web Lab Viewer Pro.

molecular tunnel was tested by the construction of mutants that were designed to disrupt the flow of molecules through this tunnel. A variety of factors were considered in the selection of residues for structural modification. To avoid secondary structural perturbations to the catalytic residues found within each of the two domains, residues located close to either of the two active sites were eliminated as candidates for mutagenesis. The side chains of the residues that orient toward the inside of the carbamate tunnel were preferred over residues whose side chains point outward from the tunnel (Val-19, Gln-22, Arg-571, and Gln-574). Consequently, four residues (Gly-21, Ala-23, Met-378, and Gly-575) were chosen as the initial targets for the implementation of structural defects within the carbamate tunnel. Seven single mutants and three double mutants were constructed and their kinetic properties measured. The direct detection of the carbamate intermediate with CPS is not possible due to the instability of carbamate. Therefore, success in blocking the carbamate tunnel was ascertained by monitoring the kinetic properties for the overall synthesis of carbamoyl phosphate in correlation with the partial reactions of the individual catalytic sites.

Met-378 was mutated to arginine in an attempt to block the carbamate tunnel by increasing the length of the side chain. The M378R mutant had a reduced bicarbonate-dependent ATPase activity (0.06 s^{-1}) compared to that of the wild-type enzyme (0.44 s^{-1}). Unfortunately, there was no additional activation of ATP turnover in the presence of glutamine (data not shown). On the basis of the proximity of this residue to the active site,² it is highly likely that the introduction of an arginine residue at this location has perturbed the active site in the carboxy phosphate domain. Further mutations at this position were not pursued.

The backbone of Gly-21 forms part of the interior lining of the carbamate tunnel. The mutation of this residue to either serine or asparagine did not diminish the partial ATP synthesis reaction activity, and thus, the catalytic machinery within the carbamoyl phosphate domain was not disrupted (Table 2). The slight diminution in the enhancement of ATP

² The side chain of Met-378 is 5.0 \AA from the γ -phosphate of AMP-PNP bound to the active site within the carboxy phosphate domain of carbamoyl phosphate synthetase.

Table 2: Kinetic Properties of Mutant and Wild-Type CPS

	HCO ₃ ⁻ - dependent ATPase	glutamine-dependent ATPase		NH ₃ -dependent ATPase		ATP synthesis		carbamoyl phosphate synthesis
	<i>k</i> _{cat} (s ⁻¹)	<i>k</i> _{cat} (s ⁻¹)	<i>K</i> _{Gln} (mM)	<i>k</i> _{cat} (s ⁻¹)	<i>K</i> _{NH₄Cl} (mM)	<i>k</i> _{cat} (s ⁻¹)	<i>K</i> _{ADP} (μM)	<i>k</i> _{cat} (s ⁻¹)
wild type	0.44 ± 0.01	6.0 ± 0.2 (α = 13.6) ^a	0.12 ± 0.01	5.2 ± 0.2 (α = 11.8)	140 ± 10	0.45 ± 0.03	16 ± 2	2.8 ± 0.1
G21S	0.40 ± 0.01	3.0 ± 0.2 (α = 7.5)	0.13 ± 0.02	2.0 ± 0.1 (α = 5.0)	93 ± 11	0.53 ± 0.06	6.7 ± 0.4	2.1 ± 0.05
G21N	0.63 ± 0.02	2.4 ± 0.1 (α = 3.8)	0.05 ± 0.01	2.1 ± 0.1 (α = 3.3)	0.21 ± 0.01	0.44 ± 0.01	26 ± 5	0.72 ± 0.02
A23L	1.0 ± 0.1	7.2 ± 0.3 (α = 7.2)	0.15 ± 0.03	3.0 ± 0.1 (α = 3.0)	81 ± 9	0.54 ± 0.01	62 ± 6	0.51 ± 0.02
A23W	0.37 ± 0.01	0.48 ± 0.01 (α = 1.3)	0.08 ± 0.02	0.39 ± 0.01 (α = 1.1)	67 ± 19	0.32 ± 0.07	7.6 ± 0.7	<0.005 ^b
G575A	0.35 ± 0.02	4.1 ± 0.1 (α = 11.9)	0.08 ± 0.01	4.0 ± 0.2 (α = 11.4)	211 ± 34	0.33 ± 0.01	11 ± 1	2.3 ± 0.1
G575S	0.35 ± 0.01	3.5 ± 0.1 (α = 9.8)	0.08 ± 0.01	2.7 ± 0.1 (α = 7.6)	201 ± 18	0.36 ± 0.01	22 ± 3	0.95 ± 0.04
G575L	0.14 ± 0.01	2.0 ± 0.1 (α = 14.4)	0.56 ± 0.07	1.7 ± 0.3 (α = 12.1)	540 ± 170	0.28 ± 0.01	71 ± 7	0.06 ± 0.01
A23L/G575A	0.63 ± 0.01	4.0 ± 0.1 (α = 6.3)	0.11 ± 0.01	1.9 ± 0.1 (α = 2.9)	99 ± 23	0.17 ± 0.01	19 ± 3	0.30 ± 0.02
A23L/G575S	0.95 ± 0.03	3.8 ± 0.1 (α = 4.0)	0.16 ± 0.02	3.0 ± 0.1 (α = 3.1)	85 ± 18	0.20 ± 0.01	38 ± 5	0.064 ± 0.006
A23L/G575L	0.18 ± 0.01	1.8 ± 0.1 (α = 10.1)	0.11 ± 0.01	0.69 ± 0.02 (α = 3.8)	23 ± 3	0.10 ± 0.01	270 ± 40	<0.005 ^b

^a α is an activation constant in ATPase activity for activation by a nitrogen source compared to the bicarbonate-dependent ATPase assay. ^b Detection limit.

Table 3: Multiple Sequence Alignments of Amino Acids that Constitute a Portion of the Carbamate Tunnel from Bacteria, Plants, Humans, Fruit Flies, and Yeast^a

	18	26	52	378	383	570	578	604	911	916
<i>E. coli</i> K12	---IVIGQACEF---	A---	MKSVGE---	NRIGQGI	EF---	E---	MRSTGE---			
<i>Arabidopsis thaliana</i>	---IVIGQACEF---	A---	MKSVGE---	NRIGQGI	EF---	E---	MRSTGE---			
<i>Homo sapiens</i>	---LSIGQACEF---	A---	MKSVGE---	YRIGSSVEF---	E---	WTSTGE---				
<i>Drosophila melanogaster</i>	---LSIGQACEF---	A---	MKSVGE---	YRIGSSVEF---	E---	WTSTGE---				
<i>Saccharomyces cerevisiae</i>	---LSIGQACEF---	A---	MKSVGE---	YRIGSSVEF---	E---	MASTGE---				

^a Letters with a black background represent residues that are very highly conserved in both prokaryotes and eukaryotes. Letters with a white background represent residues that are weakly conserved in the carbamate tunnel (V19, F26, A52, and R912 in *E. coli*).

turnover by added glutamine (reflected by α in Table 2) indicates that there were only minor alterations to the coupling of glutamine hydrolysis and bicarbonate phosphorylation. The rate of carbamoyl phosphate formation by the mutant G21S is essentially the same as that of the wild-type enzyme. However, G21N exhibited a 4-fold decrease in the rate of glutamine-dependent carbamoyl phosphate synthesis. The reduction in the rate of carbamoyl phosphate formation may have resulted from the blockage of the carbamate tunnel, but the ratio of the extent of ADP to carbamoyl phosphate formation increased to only ~3:1. Therefore, if the diffusion of carbamate through this tunnel is diminished by these mutations, it has not been enough to be kinetically significant.

The side chain of Ala-23 projects toward the inside of the carbamate tunnel (Figure 2). This residue was altered to leucine and tryptophan to impose a steric barrier for the passage of carbamate within the tunnel. The kinetic constants for the partial ATP synthesis reaction showed no substantial change for the mutants A23L and A23W, relative to those for the wild-type enzyme. However, A23W displayed a considerable decrease in the rate of ATP hydrolysis in the presence of glutamine, and thus, there was no enhancement in rate, compared to the rate of bicarbonate-dependent ATP turnover. This observation implies that the site for the phosphorylation of bicarbonate has been structurally perturbed and unresponsive to the addition of ammonia. The A23L mutant exhibits ATPase activity comparable to that of the wild-type enzyme, with a reasonable activation in the presence of glutamine. The rate of carbamoyl phosphate synthesis is ~5-fold smaller than the wild-type activity. The kinetic data suggest that this decrease in rate results from the inefficient supply of carbamate to the carbamoyl phos-

phate domain rather than from a malfunction in either active site.

The last residue to be mutated was Gly-575. This residue is more than 20 Å away from the active site for bicarbonate phosphorylation and ~14 Å away from the carbamoyl phosphate binding site. The structural integrity of the carbamoyl phosphate binding site in the C-terminal domain was tested using the partial ATP synthesis assay, which is independent of other partial reactions. Gly-575 is positionally homologous to Ala-23 (Table 1). On the basis of the dimensions of the carbamate tunnel in the vicinity of this residue, a side chain larger than leucine would appear to be too big to fit without disruption of the surrounding residues. Consequently, a series of single mutants (G575A, G575S, and G575L) were constructed in an attempt to titrate the size of side chain that could be accommodated before the active site structures were structurally perturbed. The overall kinetic properties of G575A are very similar to those of the wild-type protein, while those of G575S are only slightly perturbed. The mutant G575L has approximately one-third of the bicarbonate-dependent ATPase activity of the wild-type enzyme, although the activation of ATP turnover by glutamine and ammonia is very similar to that observed with the wild-type enzyme. The mutant G575L had a substantial drop in the rate of carbamoyl phosphate synthesis (0.055 s⁻¹), while the rate of the partial back reaction was only slightly diminished relative to that of the wild-type enzyme. The ratio of glutamine-dependent ATPase turnover to the rate of carbamoyl phosphate synthesis is ~2.1 for the wild type, and increases to 3.7 and 37 for G575S and G575L, respectively (Figure 5). Collectively, these data are consistent with an inefficient passage of carbamate through the tunnel

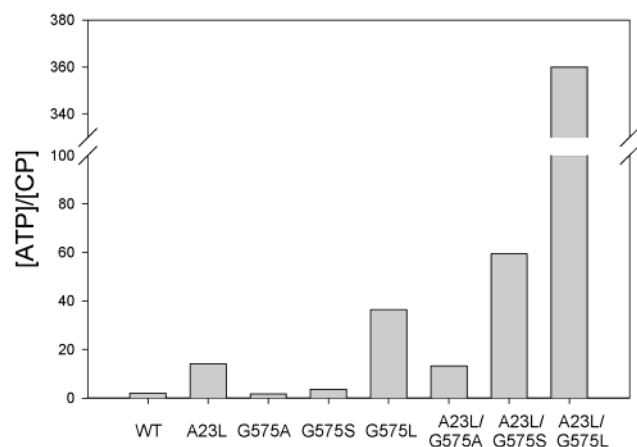


FIGURE 5: Ratio of the amount of ATP hydrolyzed to the amount of carbamoyl phosphate synthesized per unit time for the wild type and various mutants within the carbamate tunnel of CPS.

to a degree that correlates with the size of the side chain used as a replacement for glycine.

A series of double mutants containing alterations at Ala-23 and Gly-575 were constructed in an attempt to block the carbamate tunnel with even greater efficiency. The mutant A23L/G575A displayed a moderate change in catalytic properties where the rate of carbamoyl phosphate synthesis decreases by a factor of ~ 2 relative to that of the A23L mutant (Table 2). The A23L/G575S mutant had a substantial turnover of ATP, but the carbamoyl phosphate synthesis rate decreased by more than 40-fold relative to that of the wild-type enzyme. Finally, in the case of the A23L/G575L mutant, the carbamoyl phosphate synthesis rate is undetectable but the rate of the turnover of ATP is reduced by a factor of only 3 compared to that of the wild-type protein. The ratio of the glutamine-dependent ATPase rate to the carbamoyl phosphate synthesis rate is 13, 60, and >360 for the three double mutants. With the A23L/G575L mutant, the catalytic machinery at all three active site works reasonably well but no carbamoyl phosphate is made. However, it should be noted that the value of k_{cat}/K_m for the A23L/G575L mutant in the partial back reaction has been reduced by a factor of ~ 75 , relative to that of the wild-type enzyme. This reduction in catalytic efficiency is larger than the product of the observed effects for the two single-site mutants. The distance between the α -carbons of A23 and G575 is ~ 9.5 Å, and thus, there may be some cooperative interference upon mutation of both sites simultaneously. Nevertheless, these results are fully consistent with the effective blockage of the tunnel for the passage of carbamate from one active site to the next.

Although the steady-state rate constants for some of the mutants described in this study do not appear to differ significantly from that of the wild-type enzyme, the microscopic rate of carbamate transfer through the tunnel may have been substantially reduced. The decreased rate of migration may have been masked by a slower rate-determining step, which has not been clearly identified for the wild-type CPS (14). A crude estimate of the rate constant for a one-dimensional diffusion of carbamate through a 31 Å tunnel is $3 \times 10^4 \text{ s}^{-1}$ (15). If this estimate is close to reality, then the blockage of the carbamate tunnel will not be able to be

detected by steady-state rate measurements until the rate of diffusion through the tunnel becomes attenuated by approximately 3 orders of magnitude.

The reaction rates of the three active sites are highly synchronized in wild-type CPS. In most of the carbamate tunnel mutants, the activation of ATP turnover by the hydrolysis of glutamine is perturbed only moderately. The ATP turnover for the A23L/G575L mutant is activated 10-fold in the presence of glutamine, but there is no formation of carbamoyl phosphate. Therefore, the double mutant has not inhibited the synchronization of the catalytic activities possessed by the small subunit and the site for the phosphorylation of bicarbonate. These results are reminiscent of the results observed with a series of mutants designed to block the passage of ammonia through the *ammonia tunnel*. With these mutants, the signal transduction between the small and large subunits remained intact and the rate of glutamine hydrolysis was comparable to that of the wild type in the channel-impaired mutants, G359Y and G359F (6). These mutants were able to use ammonia as a nitrogen source during the synthesis of carbamoyl phosphate.

Some Other Enzymes with Tunnels. Tryptophan synthase was the first enzyme shown to contain a molecular tunnel by X-ray crystallography (16). The α -subunit catalyzes the cleavage of indole 3-glycerol phosphate (IGP) to indole and glyceraldehyde 3-phosphate (G3P), whereas the β -subunit catalyzes the condensation of indole and serine (17). Transfer of indole from the α -subunit to the β -subunit through a molecular tunnel that is 25 Å in length has been experimentally supported by kinetic characterization of channel-impaired mutants, where Cys-170 was modified to the bulkier phenylalanine (β C170F) or tryptophan (β C170W) (18). In β C170F, the channeling rate of indole decreased by more than 1 order of magnitude whereas communication between the α - and β -subunits appeared to be operative. However, in the β C170W mutant, the channeling rate was reduced more than 1000-fold and the intersubunit coupling became impaired.

Glutamine phosphoribosylpyrophosphate amidotransferase (GPATase) has a molecular tunnel for facilitating the transport of ammonia from the glutamine domain to the PRPP domain, which are 20 Å apart (19). Binding of PRPP lowers the K_m for glutamine 100-fold, and increases V_{max} approximately 3-fold (20). Interestingly, the existence of the molecular tunnel appears to be transient, unlike CPS and tryptophan synthase. The enzyme exists either in an *open* conformation where the two active sites are approximately 16 Å apart and mostly solvent accessible or in a *closed* conformation, which is an active form of the enzyme (19–21). Binding of PRPP triggers a conformational change from an open conformation to the closed one by closing a flexible loop in the PRPP domain, which forms the ammonia tunnel. The kinetic characterization of the molecular tunnel has been achieved through construction of *leaky* tunnel mutants, where an amino acid lining the ammonia tunnel has been altered to one that has a smaller side chain resulting in a *hole* in the wall of the tunnel. These mutants release ammonia into the bulk solvent and reduce the rate of synthesis of PRA within the PRPP domain (21). In GPATase, channeling efficiency is closely related to interdomain signal transduction since most of the leaky mutants exhibited a higher K_m for glutamine.

ACKNOWLEDGMENT

We thank Professor Hazel M. Holden for many useful discussions.

REFERENCES

1. Anderson, P. M., and Meister, A. (1966) *Biochemistry* 5, 3157–3163.
2. Anderson, P. M., and Meister, A. (1965) *Biochemistry* 4, 2803–2809.
3. Thoden, J. B., Holden, H. M., Wesenberg, G., Raushel, F. M., and Rayment, I. (1997) *Biochemistry* 36, 6305–6316.
4. Mullins, L. S., and Raushel, F. M. (1999) *J. Am. Chem. Soc.* 121, 3803–3804.
5. Huang, X., and Raushel, F. M. (2000) *Biochemistry* 39 (12), 3240–3247.
6. Huang, X., and Raushel, F. M. (2000) *J. Biol. Chem.* 275, 26233–26240.
7. Raushel, F. M., Mullins, L. S., and Gibson, G. E. (1998) *Biochemistry* 37, 10272–10278.
8. Wang, T. T., Bishop, S. H., and Himoe, A. (1972) *J. Biol. Chem.* 247, 4437–4440.
9. Stapleton, M. A., Javid-Majd, F., Harmon, M. F., Hanks, B. A., Grahmann, J. L., Mullins, L. S., and Raushel, F. M. (1996) *Biochemistry* 35, 14532–14561.
10. Mareya, S. M., and Raushel, F. M. (1994) *Biochemistry* 33, 2945–2950.
11. Snodgrass, P. J., and Parry, D. J. (1969) *J. Lab. Clin. Med.* 73, 940–950.
12. Cleland, W. W. (1970) in *The Enzymes*, 3rd ed., Vol. 2, pp 1–65, Academic Press, New York.
13. Thoden, J. B., Wesenberg, G., Raushel, F. M., and Holden, H. M. (1999) *Biochemistry* 38, 2347–2357.
14. Miles, B. W., and Raushel, F. M. (2000) *Biochemistry* 39, 5051–5056.
15. Huang, X., Holden, H. M., and Raushel, F. M. (2001) *Annu. Rev. Biochem.* 70, 149–180.
16. Hyde, C. C., Ahmed, S. A., Padlan, E. A., Miles, E. W., and Davies, D. R. (1988) *J. Biol. Chem.* 263, 17857–17871.
17. Miles, E. W. (1979) *Adv. Enzymol.* 49, 127–186.
18. Anderson, K. S., Kim, A. Y., Quillen, J. M., Sayers, E., Yang, X.-J., and Miles, E. W. (1995) *J. Biol. Chem.* 270, 29936–29944.
19. Krahn, J. M., Kim, J. H., Burns, M. R., Parry, R. J., Zalkin, H., and Smith, J. L. (1997) *Biochemistry* 36, 11061–11068.
20. Kim, J. H., Krahn, J. M., Tomchick, D. R., Smith, J. L., and Zalkin, H. (1996) *J. Biol. Chem.* 271, 15549–15557.
21. Bera, A. K., Smith, J. L., and Zalkin, H. (2000) *J. Biol. Chem.* 275, 7975–7979.

BI020421O